A space-time smooth artificial viscosity method for nonlinear conservation laws: the C-method

Steve Shkoller

Department of Mathematics
University of California, Davis

In collaboration with J. Reisner and J. Serencsa

Journal of Computational Physics, (2012)

Winter School Lecture 4

Dec 20, 2012

Systems of Nonlinear Conservation Laws

Strong and weak forms

- Conservation laws for the vector $\mathbf{u} = (u_1, ..., u_m)$ and flux $F(\mathbf{u})$:

$$\begin{aligned} \mathbf{u}_t + \operatorname{div} F(\mathbf{u}) &= 0\,, && t > 0\,,\ x \in \Omega \subset \mathbb{R}^D \\ \mathbf{u}(x,0) &= \mathbf{u}_0(x) && x \in \Omega \subset \mathbb{R}^D \end{aligned}$$

- In 1-D,

$$\begin{aligned} \mathbf{u}_t + F(\mathbf{u})_x &= 0\,, && t > 0\,,\ x \in \mathcal{I} \subset \mathbb{R} \\ \mathbf{u}(x,0) &= \mathbf{u}_0(x) && x \in \mathcal{I} \subset \mathbb{R} \end{aligned}$$

Definition (Weak solution)

A bounded vector $\mathbf{u}(x,t)$ is an integral solution if

$$\int_0^\infty \int_{\mathcal{I}} \mathbf{u} \cdot \phi_t + F(\mathbf{u}) \cdot \phi_x \, dxdt + \int_{\mathcal{I}} \mathbf{u}_0(x) \cdot \phi(x,0) dx = 0$$

for all smooth test function $\phi : \mathcal{I} \times [0,\infty) \to \mathbb{R}^m$ with compact support.

- Physically relevant solutions require an additional entropy condition.

Systems of Nonlinear Conservation Laws

Strong and weak forms

- Conservation laws for the vector $\mathbf{u} = (u_1, ..., u_m)$ and flux $F(\mathbf{u})$:

$$\mathbf{u}_t + \operatorname{div} F(\mathbf{u}) = 0\,, \qquad t > 0\,,\ x \in \Omega \subset \mathbb{R}^D$$
$$\mathbf{u}(x,0) = \mathbf{u}_0(x) \qquad x \in \Omega \subset \mathbb{R}^D$$

- In 1-D,

$$\mathbf{u}_t + F(\mathbf{u})_x = 0\,, \qquad t > 0\,,\ x \in \mathcal{I} \subset \mathbb{R}$$
$$\mathbf{u}(x,0) = \mathbf{u}_0(x) \qquad x \in \mathcal{I} \subset \mathbb{R}$$

Definition (Weak solution)

A bounded vector $\mathbf{u}(x,t)$ is an integral solution if

$$\int_0^\infty \int_{\mathcal{I}} \mathbf{u} \cdot \phi_t + F(\mathbf{u}) \cdot \phi_x \, dxdt + \int_{\mathcal{I}} \mathbf{u}_0(x) \cdot \phi(x,0) dx = 0$$

for all smooth test function $\phi : \mathcal{I} \times [0,\infty) \to \mathbb{R}^m$ with compact support.

- Physically relevant solutions require an additional entropy condition.

Systems of Nonlinear Conservation Laws

Strong and weak forms

- Conservation laws for the vector $\mathbf{u} = (u_1, ..., u_m)$ and flux $F(\mathbf{u})$:

$$\mathbf{u}_t + \operatorname{div} F(\mathbf{u}) = 0\,, \qquad t > 0\,,\ x \in \Omega \subset \mathbb{R}^D$$
$$\mathbf{u}(x, 0) = \mathbf{u}_0(x) \qquad x \in \Omega \subset \mathbb{R}^D$$

- In 1-D,

$$\mathbf{u}_t + F(\mathbf{u})_x = 0\,, \qquad t > 0\,,\ x \in \mathcal{I} \subset \mathbb{R}$$
$$\mathbf{u}(x, 0) = \mathbf{u}_0(x) \qquad x \in \mathcal{I} \subset \mathbb{R}$$

Definition (Weak solution)

A bounded vector $\mathbf{u}(x, t)$ is an integral solution if

$$\int_0^\infty \int_{\mathcal{I}} \mathbf{u} \cdot \phi_t + F(\mathbf{u}) \cdot \phi_x \, dxdt + \int_{\mathcal{I}} \mathbf{u}_0(x) \cdot \phi(x, 0) dx = 0$$

for all smooth test function $\phi : \mathcal{I} \times [0, \infty) \to \mathbb{R}^m$ with compact support.

- Physically relevant solutions require an additional entropy condition.

The Compressible Euler Equations

The Eulerian formulation in 1-D

- $\mathbf{u} = (m, \rho, E)$ satisfies

$$m_t + \left(\frac{m^2}{\rho} + p\right)_x = 0 \qquad \text{(Conservation of Momentum)}$$

$$\rho_t + m_x = 0 \qquad \text{(Conservation of Mass)}$$

$$E_t + \left(\frac{m}{\rho}(E + p)\right)_x = 0 \qquad \text{(Conservation of Energy)}$$

with equation of state

$$p = (\gamma - 1)\left(E - \frac{m^2}{2\rho}\right) = (\gamma - 1)\rho e\,,$$

where the internal energy satisfies

$$e_t + e_x u + (\gamma - 1) e u_x = 0\,.$$

- For smooth solutions, E-eqn can be replaced by $S_t + S_x u = 0$.

The Compressible Euler Equations

The Eulerian formulation in 1-D

- $\mathbf{u} = (m, \rho, E)$ satisfies

$$m_t + \left(\frac{m^2}{\rho} + p\right)_x = 0 \qquad \text{(Conservation of Momentum)}$$

$$\rho_t + m_x = 0 \qquad \text{(Conservation of Mass)}$$

$$E_t + \left(\frac{m}{\rho}(E+p)\right)_x = 0 \qquad \text{(Conservation of Energy)}$$

  with equation of state

$$p = (\gamma - 1)\left(E - \frac{m^2}{2\rho}\right) = (\gamma - 1)\rho e\,,$$

  where the internal energy satisfies

$$e_t + e_x u + (\gamma - 1) e u_x = 0\,.$$

- For smooth solutions, E-eqn can be replaced by $S_t + S_x u = 0$.

The Artificial Viscosity of Richtmyer and Von Neumann

- Richtmyer (1948) and VonNeumann & Richtmyer(1950) introduced artificial viscosity in gas dynamics in Lagrangian variables
- With $\eta(x, t)$ the position of particle x at time t, the density $\rho \circ \eta = \frac{\rho_0}{\eta_x}$
- The Euler equations in Lagrangian variables are given by

$$\rho_0 U_t + P_x = 0 \quad \text{and} \quad \mathcal{E}_t + \frac{P}{\rho} U_x = 0 \,.$$

- With $\epsilon = \Delta x$, they introduced

$$\rho_0 U_t + P_x = \beta \epsilon^2 (\rho |U_x| U_x)_x \quad \text{and} \quad \mathcal{E}_t + \frac{P}{\rho} U_x = \beta \epsilon^2 \rho |U_x| U_x^2 \,.$$

- The mass equation was unchanged
- Modulo the coefficient $|U_x|$, the RvN artificial viscosity is similar to the viscosity of a real fluid (more later)
- Lax (1954) noted that the magnitude of this viscosity is too large to be justified.

The Artificial Viscosity of Richtmyer and Von Neumann

- Richtmyer (1948) and VonNeumann & Richtmyer(1950) introduced artificial viscosity in gas dynamics in Lagrangian variables
- With $\eta(x,t)$ the position of particle x at time t, the density $\rho \circ \eta = \frac{\rho_0}{\eta_x}$
- The Euler equations in Lagrangian variables are given by

$$\rho_0 U_t + P_x = 0 \quad \text{and} \quad \mathcal{E}_t + \frac{P}{\rho} U_x = 0 \,.$$

- With $\epsilon = \Delta x$, they introduced

$$\rho_0 U_t + P_x = \beta\epsilon^2(\rho|U_x|U_x)_x \quad \text{and} \quad \mathcal{E}_t + \frac{P}{\rho} U_x = \beta\epsilon^2\rho|U_x|U_x^2 \,.$$

- The mass equation was unchanged
- Modulo the coefficient $|U_x|$, the RvN artificial viscosity is similar to the viscosity of a real fluid (more later)
- Lax (1954) noted that the magnitude of this viscosity is too large to be justified.

The Artificial Viscosity of Richtmyer and Von Neumann

- Richtmyer (1948) and VonNeumann & Richtmyer(1950) introduced artificial viscosity in gas dynamics in Lagrangian variables
- With $\eta(x,t)$ the position of particle x at time t, the density $\rho \circ \eta = \frac{\rho_0}{\eta_x}$
- The Euler equations in Lagrangian variables are given by

$$\rho_0 U_t + P_x = 0 \quad \text{and} \quad \mathcal{E}_t + \frac{P}{\rho} U_x = 0\,.$$

- With $\epsilon = \Delta x$, they introduced

$$\rho_0 U_t + P_x = \beta \epsilon^2 (\rho |U_x| U_x)_x \quad \text{and} \quad \mathcal{E}_t + \frac{P}{\rho} U_x = \beta \epsilon^2 \rho |U_x| U_x^2\,.$$

- The mass equation was unchanged
- Modulo the coefficient $|U_x|$, the RvN artificial viscosity is similar to the viscosity of a real fluid (more later)
- Lax (1954) noted that the magnitude of this viscosity is too large to be justified.

The Artificial Viscosity of Richtmyer and Von Neumann

- Richtmyer (1948) and VonNeumann & Richtmyer(1950) introduced artificial viscosity in gas dynamics in Lagrangian variables
- With $\eta(x,t)$ the position of particle x at time t, the density $\rho \circ \eta = \frac{\rho_0}{\eta_x}$
- The Euler equations in Lagrangian variables are given by

$$\rho_0 U_t + P_x = 0 \quad \text{and} \quad \mathcal{E}_t + \frac{P}{\rho} U_x = 0\,.$$

- With $\epsilon = \Delta x$, they introduced

$$\rho_0 U_t + P_x = \beta\epsilon^2 (\rho |U_x| U_x)_x \quad \text{and} \quad \mathcal{E}_t + \frac{P}{\rho} U_x = \beta\epsilon^2 \rho |U_x| U_x^2\,.$$

- The mass equation was unchanged
- Modulo the coefficient $|U_x|$, the RvN artificial viscosity is similar to the viscosity of a real fluid (more later)
- Lax (1954) noted that the magnitude of this viscosity is too large to be justified.

The Artificial Viscosity of Richtmyer and Von Neumann

- Richtmyer (1948) and VonNeumann & Richtmyer(1950) introduced artificial viscosity in gas dynamics in Lagrangian variables
- With $\eta(x,t)$ the position of particle x at time t, the density $\rho \circ \eta = \frac{\rho_0}{\eta_x}$
- The Euler equations in Lagrangian variables are given by

$$\rho_0 U_t + P_x = 0 \quad \text{and} \quad \mathcal{E}_t + \frac{P}{\rho} U_x = 0\,.$$

- With $\epsilon = \Delta x$, they introduced

$$\rho_0 U_t + P_x = \beta \epsilon^2 (\rho |U_x| U_x)_x \quad \text{and} \quad \mathcal{E}_t + \frac{P}{\rho} U_x = \beta \epsilon^2 \rho |U_x| U_x^2\,.$$

- The mass equation was unchanged
- Modulo the coefficient $|U_x|$, the RvN artificial viscosity is similar to the viscosity of a real fluid (more later)
- Lax (1954) noted that the magnitude of this viscosity is too large to be justified.

The Artificial Viscosity of Richtmyer and Von Neumann

- Richtmyer (1948) and VonNeumann & Richtmyer(1950) introduced artificial viscosity in gas dynamics in Lagrangian variables
- With $\eta(x,t)$ the position of particle x at time t, the density $\rho \circ \eta = \frac{\rho_0}{\eta_x}$
- The Euler equations in Lagrangian variables are given by

$$\rho_0 U_t + P_x = 0 \quad \text{and} \quad \mathcal{E}_t + \frac{P}{\rho} U_x = 0\,.$$

- With $\epsilon = \Delta x$, they introduced

$$\rho_0 U_t + P_x = \beta\epsilon^2(\rho|U_x|U_x)_x \quad \text{and} \quad \mathcal{E}_t + \frac{P}{\rho} U_x = \beta\epsilon^2\rho|U_x|U_x^2\,.$$

- The mass equation was unchanged
- Modulo the coefficient $|U_x|$, the RvN artificial viscosity is similar to the viscosity of a real fluid (more later)
- Lax (1954) noted that the magnitude of this viscosity is too large to be justified.

Classical Artificial Viscosity

- Following Landshoff (1955), Lapidus (1967), Kuropatenko (1967), Wilkins (1980), and others, a general form for conservation laws with *artificial viscosity* is given by

$$\mathbf{u}_t + F(\mathbf{u})_x = \beta_1 \epsilon \, \mathbf{u}_{xx} + \beta_2 \epsilon^2 (|\mathbf{u}_x| \mathbf{u}_x)_x \, .$$

- β_i can depend on local velocity, sound speed of the material – β_1 usually *order of magnitude smaller* than β_2
- A *compression switch* following Richtmyer & Morton (1967) also used
- Artificial viscosity should maintain fundamental invariance properties and not affect uniform compression Caramana, Shashkov, & Whalen (1998)
- The diffusion coefficient $|\mathbf{u}_x|$ tends to become oscillatory, and (mathematically) prevents smoothness of solutions
- Can we produce a smooth and localized version of $|u_x|$ to use as a diffusion coefficient?

Classical Artificial Viscosity

- Following Landshoff (1955), Lapidus (1967), Kuropatenko (1967), Wilkins (1980), and others, a general form for conservation laws with *artificial viscosity* is given by

$$\mathbf{u}_t + F(\mathbf{u})_x = \beta_1 \epsilon\, \mathbf{u}_{xx} + \beta_2 \epsilon^2 (|\mathbf{u}_x| \mathbf{u}_x)_x \,.$$

- β_i can depend on local velocity, sound speed of the material – β_1 usually *order of magnitude smaller* than β_2
- A *compression switch* following Richtmyer & Morton (1967) also used
- Artificial viscosity should maintain fundamental invariance properties and not affect uniform compression Caramana, Shashkov, & Whalen (1998)
- The diffusion coefficient $|\mathbf{u}_x|$ tends to become oscillatory, and (mathematically) prevents smoothness of solutions
- Can we produce a smooth and localized version of $|u_x|$ to use as a diffusion coefficient?

Classical Artificial Viscosity

- Following Landshoff (1955), Lapidus (1967), Kuropatenko (1967), Wilkins (1980), and others, a general form for conservation laws with *artificial viscosity* is given by

$$\mathbf{u}_t + F(\mathbf{u})_x = \beta_1 \epsilon \, \mathbf{u}_{xx} + \beta_2 \epsilon^2 (|\mathbf{u}_x| \mathbf{u}_x)_x \, .$$

- β_i can depend on local velocity, sound speed of the material – β_1 usually *order of magnitude smaller* than β_2
- A *compression switch* following Richtmyer & Morton (1967) also used
- Artificial viscosity should maintain fundamental invariance properties and not affect uniform compression Caramana, Shashkov, & Whalen (1998)
- The diffusion coefficient $|\mathbf{u}_x|$ tends to become oscillatory, and (mathematically) prevents smoothness of solutions
- Can we produce a smooth and localized version of $|u_x|$ to use as a diffusion coefficient?

Classical Artificial Viscosity

- Following Landshoff (1955), Lapidus (1967), Kuropatenko (1967), Wilkins (1980), and others, a general form for conservation laws with *artificial viscosity* is given by

$$\mathbf{u}_t + F(\mathbf{u})_x = \beta_1 \epsilon\, \mathbf{u}_{xx} + \beta_2 \epsilon^2 (|\mathbf{u}_x| \mathbf{u}_x)_x \,.$$

- β_i can depend on local velocity, sound speed of the material – β_1 usually *order of magnitude smaller* than β_2
- A *compression switch* following Richtmyer & Morton (1967) also used
- Artificial viscosity should maintain fundamental invariance properties and not affect uniform compression Caramana, Shashkov, & Whalen (1998)
- The diffusion coefficient $|\mathbf{u}_x|$ tends to become oscillatory, and (mathematically) prevents smoothness of solutions
- Can we produce a smooth and localized version of $|u_x|$ to use as a diffusion coefficient?

Classical Artificial Viscosity

- Following Landshoff (1955), Lapidus (1967), Kuropatenko (1967), Wilkins (1980), and others, a general form for conservation laws with *artificial viscosity* is given by

$$\mathbf{u}_t + F(\mathbf{u})_x = \beta_1 \epsilon \, \mathbf{u}_{xx} + \beta_2 \epsilon^2 (|\mathbf{u}_x| \mathbf{u}_x)_x \, .$$

- β_i can depend on local velocity, sound speed of the material – β_1 usually *order of magnitude smaller* than β_2
- A *compression switch* following Richtmyer & Morton (1967) also used
- Artificial viscosity should maintain fundamental invariance properties and not affect uniform compression Caramana, Shashkov, & Whalen (1998)
- The diffusion coefficient $|\mathbf{u}_x|$ tends to become oscillatory, and (mathematically) prevents smoothness of solutions
- Can we produce a smooth and localized version of $|u_x|$ to use as a diffusion coefficient?

The C-method

- Nonlinear conservation laws with modified artificial flux:

$$\partial_t \mathbf{u}^\epsilon + \partial_x \mathbf{F}(\mathbf{u}^\epsilon) = \tilde{\beta}\epsilon^2 \partial_x \left(C^\epsilon \partial_x \mathbf{u}^\epsilon \right), \quad t > 0,$$
$$\frac{1}{S(\mathbf{u}^\epsilon)} \partial_t C^\epsilon - \gamma \epsilon \partial_x^2 C^\epsilon + \frac{1}{\epsilon} C^\epsilon = G(\partial_x u^\epsilon), \quad t > 0,$$

- $\tilde{\beta} = \beta \frac{\max_{\mathcal{I}} |\partial_x u^\epsilon|}{\max_{\mathcal{I}} C^\epsilon}$ (convenient normalization for comparison)
- $\beta = O(1)$
- Forcing function $G(\partial_x u^\epsilon) = \frac{|\partial_x u^\epsilon|}{\max_{\mathcal{I}} |\partial_x u^\epsilon|} \underbrace{\mathbf{1}_{(u_x<0)}}_{\text{Compression Switch}}$
- Max wave speed $[S(\mathbf{u})](t) = \max_{i=1,2,3} \max_{x\in\mathcal{I}} \{|\lambda_i(x,t)|\}$
- $\gamma = 1$ or γ can be taken to be *inversely proportional* to M^-

Comparison of C vs $|\mathbf{u}_x|$

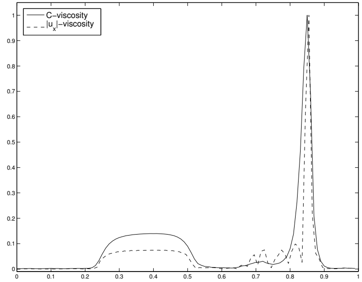

(a) Without compression switch

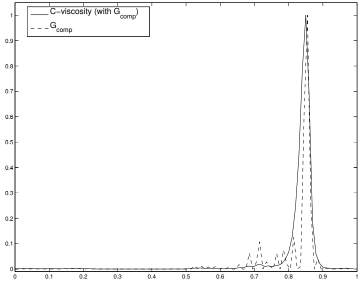

(b) With compression switch

Why does the graph of C look the way it does?

- Equilibrium solutions to the C-equation are minimizers of the following functional:

$$\mathcal{E}_G(C) = \int \left(\frac{\epsilon}{2} C_x^2 - G(u_x)C + \frac{1}{2\epsilon} C^2 \right) dx \, .$$

- With forcing function $G(u_x) = 0$, this reduces to

$$\mathcal{E}_0(C) = \frac{1}{2} \int \left(\epsilon C_x^2 + \frac{1}{\epsilon} C^2 \right) dx \, .$$

- The second term can be viewed as a *penalization of the Dirichlet energy*
- minimizers are trying to be harmonic while minimizing their support
- C-equation can be written as a classical gradient flow equation $\frac{dC}{dt} = -S(u)\nabla\mathcal{E}_G(C)$

Why does the graph of C look the way it does?

- Equilibrium solutions to the C-equation are minimizers of the following functional:

$$\mathcal{E}_G(C) = \int \left(\frac{\epsilon}{2} C_x^2 - G(u_x)C + \frac{1}{2\epsilon} C^2 \right) dx \,.$$

- With forcing function $G(u_x) = 0$, this reduces to

$$\mathcal{E}_0(C) = \frac{1}{2} \int \left(\epsilon C_x^2 + \frac{1}{\epsilon} C^2 \right) dx \,.$$

- The second term can be viewed as a *penalization of the Dirichlet energy*
- minimizers are trying to be harmonic while minimizing their support
- C-equation can be written as a classical gradient flow equation $\frac{dC}{dt} = -S(u)\nabla\mathcal{E}_G(C)$

Why does the graph of C look the way it does?

- Equilibrium solutions to the C-equation are minimizers of the following functional:

$$\mathcal{E}_G(C) = \int \left(\frac{\epsilon}{2} C_x^2 - G(u_x)C + \frac{1}{2\epsilon} C^2 \right) dx \,.$$

- With forcing function $G(u_x) = 0$, this reduces to

$$\mathcal{E}_0(C) = \frac{1}{2} \int \left(\epsilon C_x^2 + \frac{1}{\epsilon} C^2 \right) dx \,.$$

- The second term can be viewed as a *penalization of the Dirichlet energy*
- minimizers are trying to be harmonic while minimizing their support
- C-equation can be written as a classical gradient flow equation $\frac{dC}{dt} = -S(u)\nabla\mathcal{E}_G(C)$

FEM-C Implementation

Sod shock tube

- 2nd-order continuous-Galerkin finite-element scheme
  - spatial discretization based on piecewise second-order Lagrange polynomials
  - implicit 2nd-order time-stepping (implicit RK2)
  - Fully nonlinear Newton iteration (faster than quadratic convergence)
- Sod shock tube experiment: FEM-C vs FEM with classical artificial viscosity at t=.2

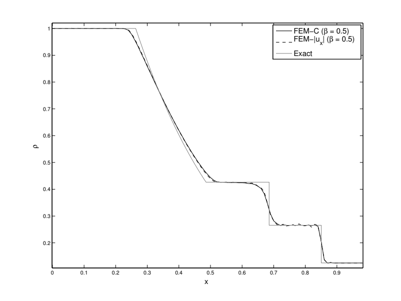

(c) Complete density profile

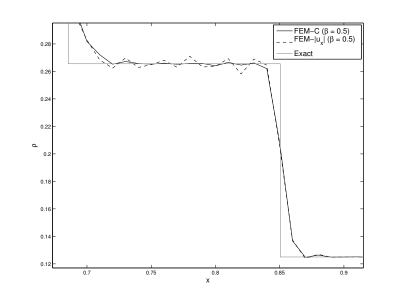

(d) Zoom-in at shock

FEM-C: Sod Shock Continued

C vs $|u_x|$

- For similar smoothness using $|u_x|$-diffusion coefficient, we need *six time as much viscosity*:

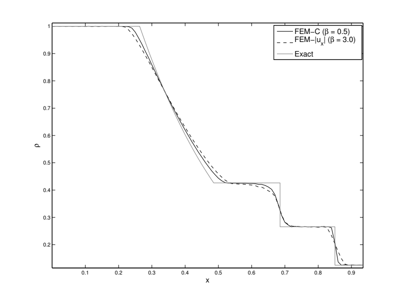

(e) Complete density profile

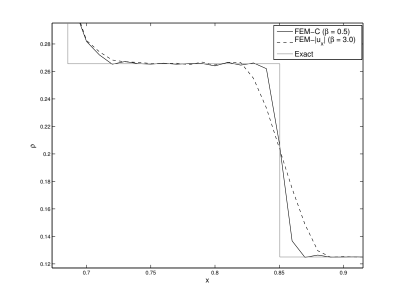

(f) Zoom-in at shock

Figure 1: Comparison of FEM-C and FEM-$|u_x|$, for the Sod shock-tube experiment with $N = 100$, $T = 0.2$. $\beta = 0.5$ for FEM-C and $\beta = 3.0$ for FEM-$|u_x|$.

- Classical artificial viscosity smears shock across too many cells

FEM-C: Sod Shock Continued

FEM-C vs NT and FEM-C vs WENO-G

- NT (Nessyahu and Tadmor): 2nd-order, consistent, conservative, monotone scheme with no Riemann solvers – uses UNO limiter
- WENO-G: 5th-order WENO with Godunov solver of Rider, Greenough, & Kamm

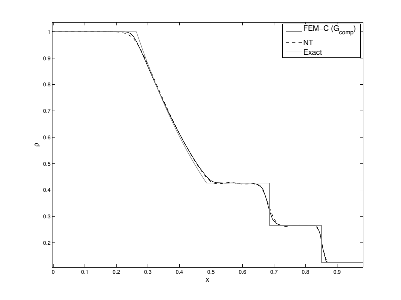

(a) FEM-C vs. NT

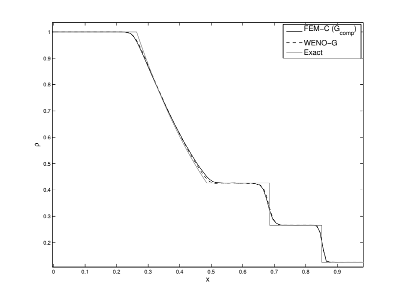

(b) FEM-C vs. WENO-G

The Osher-Shu Shock Tube Experiment

- Initial Conditions: $\begin{pmatrix} \rho_0(x) \\ m_0(x) \\ E_0(x) \end{pmatrix} = \begin{pmatrix} 3.857143 \\ 10.14185 \\ 39.1666 \end{pmatrix} \mathbf{1}_{[-1,-0.8)}(x) + \begin{pmatrix} 1 + 0.2\sin(5\pi x) \\ 0 \\ 2.5 \end{pmatrix} \mathbf{1}_{[-0.8,1]}(x)$
- Interaction of a sinusoidal entropy wave with a shock wave
- The goal is to sharply resolve the shock without damping the amplitude of sinusoidal oscillations

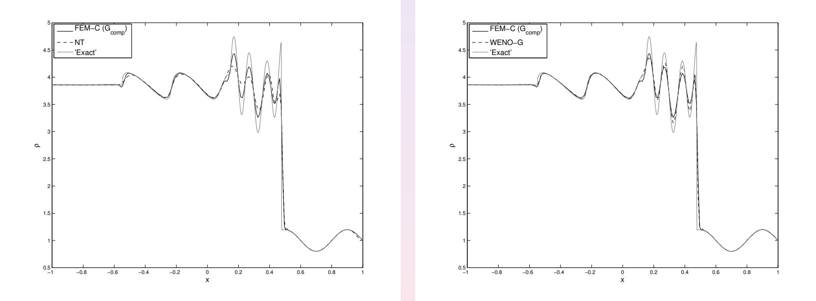

(c) FEM-C vs. NT

(d) FEM-C vs. WENO

Figure 2: Comparisons of FEM-C against NT and WENO schemes, for the Osher-Shu shock-tube experiment with $N = 200$ and $T = 0.36$.

Quantitative convergence studies

Refining the mesh for Sod and Osher-Shu

- L^1 error: $\|w - w^{exact}\|_{L^1} = \frac{1}{N}\sum_{i=1}^{N} |w_i - w_i^{exact}|$
- Greenough-Rider L^1 error $\|w - w^{exact}\|_{L^1_{G.R.}} = \frac{1}{N}\sum_{i=1}^{N} \frac{|w_i - w_i^{exact}|}{|w_i^{exact}|}$

Table 1: L^1-error Table: FEM-C for Sod Shock Tube

N	L^1-error ($\|u_x\|$)	Order	L^1-error (C)	Order
100	6.765e-3	–	6.766e-3	–
200	3.4531e-3	0.97	3.365e-3	1.00
400	1.835e-3	0.91	1.752e-3	0.94
800	9.992e-4	0.87	9.362e-4	0.90

Table 2: L^1-error: FEM-C for Osher-Shu. 'Exact" is 25, 600-cell WENO-LF

N	L^1-error	Rate
100	8.988e-2	–
200	4.686e-2	0.93
400	2.310e-2	1.02
800	1.023e-2	1.18

The WENO-C Scheme

Simple 5th-order WENO scheme together with the *C*-method

- advection terms: sign *u* chooses WENO-reconstruction
- pressure terms: higher-order centered differencing
- *artificial flux term* added only to momentum equation

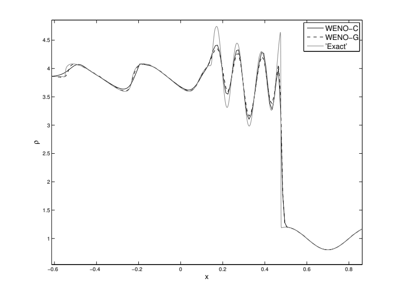

(a) WENO-C vs. WENO-G

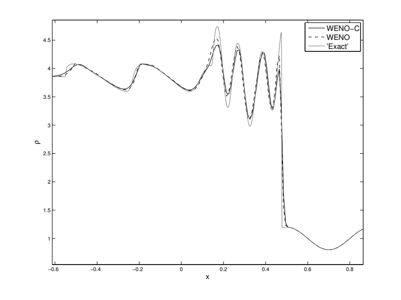

(b) WENO-C vs. WENO

- Initial Conditions:
  $\rho_0(x) = 1, \quad m_0(x) = 0, \quad E_0(x) = 250 \cdot \mathbf{1}_{[0.9,1]} + 0.25 \cdot \mathbf{1}_{[0.1,0.9)} + 2500 \cdot \mathbf{1}_{[0,0.1)}$
- A fairly difficult test case – 2nd-order schemes do *not* do so well

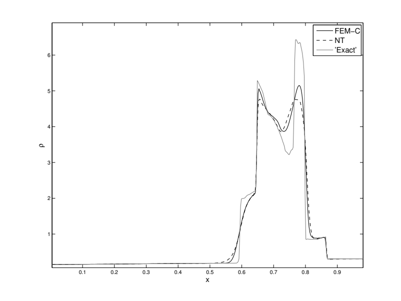

(c) FEM-C vs. NT

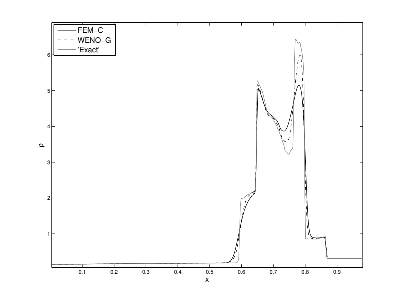

(d) FEM-C vs. WENO-G

Figure 3: Comparisons of FEM-C against NT and WENO-G schemes, for the Woodward-Colella blast-tube experiment with $N = 400$ and $T = 0.038$.

The Woodward-Colella Blast Wave Problem

Our simple WENO scheme with and without the C-method

- The C-method works well with simple WENO

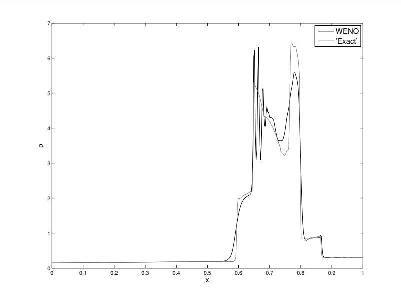

(a) Simple WENO without C

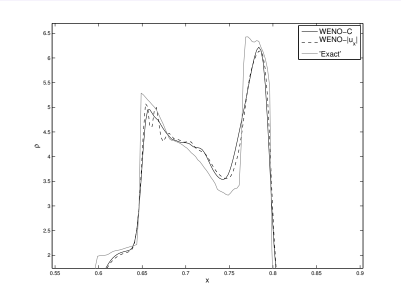

(b) WENO-C vs WENO-$|u_x|$

Figure 4: Simple WENO with and without C-method applied to the Woodward-Colella blast-tube experiment with $N = 400$ and $T = 0.038$.

The Woodward-Colella Blast Wave Problem

A comparison of WENO-C vs WENO-G

- WENO-C and WENO-G (with Godunov solver) are pretty similar for W-C

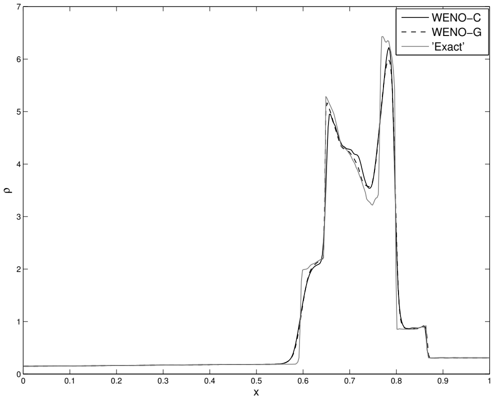

Figure 5: Comparison of WENO-C against WENO-G, for the Woodward-Colella blast-tube experiment with $N = 400$ and $T = 0.038$.

Quantitative convergence studies for WENO-C

Refining the mesh for Woodward-Colella Blast Wave

Table 3: L^1-error Table: Woodward-Colella Blast Wave

N	L^1-error (WENO-C)	Order	L^1-error (WENO-G)	Order
200	1.324e-1	–	1.256e-1	–
400	7.606e-2	0.80	7.071e-2	0.83
800	4.432e-2	0.78	4.24e-2	0.74
1600	2.471e-2	0.84	–	–

The Leblanc Shock-Tube Experiment

Strategy One: WENO-C with C_E

- Initial Conditions: $\begin{pmatrix} \rho_0(x) \\ m_0(x) \\ E_0(x) \end{pmatrix} = \begin{pmatrix} 1 \\ 0 \\ 10^{-1} \end{pmatrix} \mathbf{1}_{[0,3)}(x) + \begin{pmatrix} 10^{-3} \\ 0 \\ 10^{-9} \end{pmatrix} \mathbf{1}_{[3,9]}(x)$
- Numerically challenging experiment
  - Overshoot for the internal energy e at contact discontinuity
  - Inaccurate shock speeds
- We add a C_E-equation forced by $|\partial_x(E/\rho)|/\max|\partial_x(E/\rho)|$ in expansive region

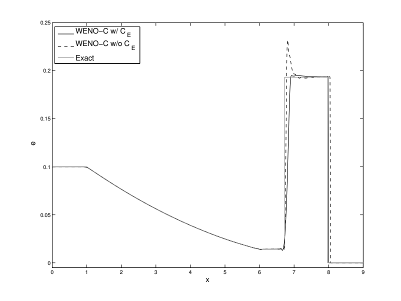

(a) With and without C_E, $N = 1440$

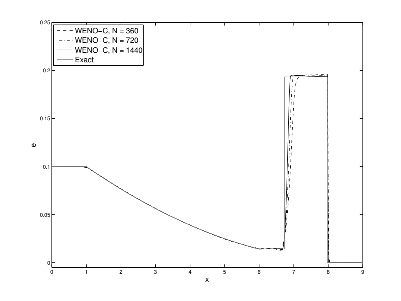

(b) $\beta_u = 1$, $\beta_E = .15$

Figure 6: Internal energy for Leblanc shock-tube experiment at $T = 6$.

Convergence studies for WENO-C with and without C_E

Refining the mesh for Leblanc Shock Tube

Table 4: L^1-error Table: Leblanc Shock Tube

N	L^1-error	Order
360	7.404e-3	–
720	4.452e-3	0.73
1440	2.491e-3	0.84

The Leblanc Shock-Tube Experiment

Strategy Two: WENO with Lax-Friedrichs Flux and the C-Method

- We return to using one C-equation forced by $|u_x|/\max|u_x|$ in compression
- WENO-LF has some dissipation – momentum equation does not require viscosity
- We only modify the energy equation and add $-\epsilon^2\beta \max u_x / \max C\, \rho|u_x|^2$ to the LHS

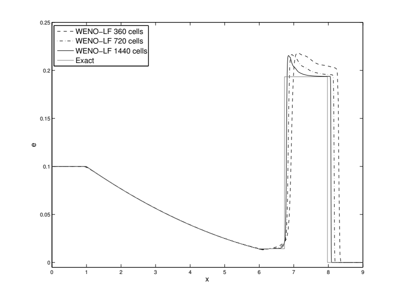

(a) WENO-LF

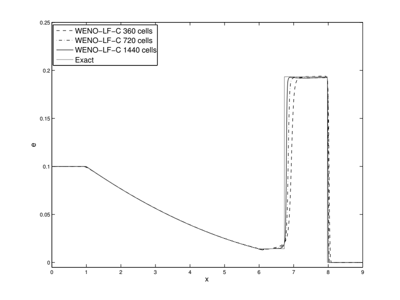

(b) WENO-LF-C

- C-method corrects the shock speed and removes overshoot of the L-F flux

The Leblanc Shock-Tube Experiment

Strategy Two: WENO with Lax-Friedrichs Flux and the C-Method

- We return to using one C-equation forced by $|u_x|/\max|u_x|$ in compression
- WENO-LF has some dissipation – momentum equation does not require viscosity
- We only modify the energy equation and add $-\epsilon^2\beta \max u_x / \max C\, \rho|u_x|^2$ to the LHS

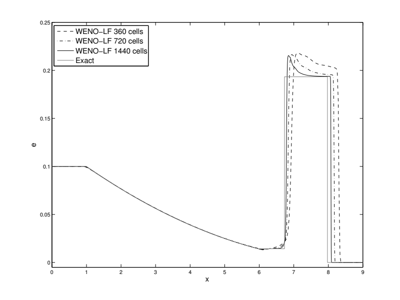

(c) WENO-LF

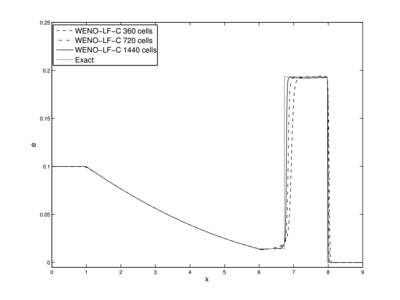

(d) WENO-LF-C

- C-method corrects the shock speed and removes overshoot of the L-F flux

The Leblanc Shock-Tube Experiment

Strategy Two: WENO with Lax-Friedrichs Flux and the C-Method

- We return to using one C-equation forced by $|u_x|/\max|u_x|$ in compression
- WENO-LF has some dissipation – momentum equation does not require viscosity
- We only modify the energy equation and add $-\epsilon^2\beta \max u_x / \max C\, \rho|u_x|^2$ to the LHS

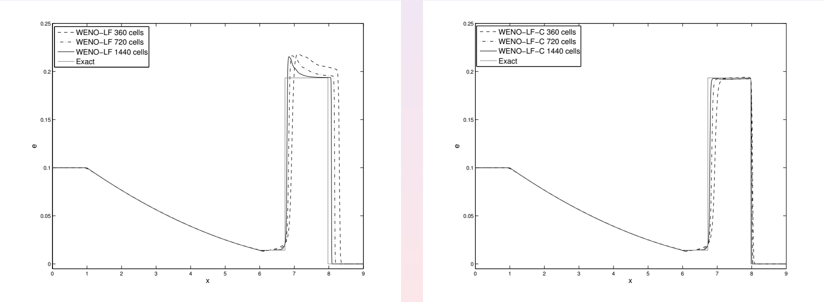

(e) WENO-LF

(f) WENO-LF-C

- C-method corrects the shock speed and removes overshoot of the L-F flux

Convergence studies for WENO-LF and WENO-LF-C

Refining the mesh for Leblanc Shock Tube

Table 5: L^1-error Table: Leblanc Shock Tube

N	L^1-error (WENO-LF-C)	Order	L^1-error (WENO-LF)	Order
360	5.382e-3	–	1.319e-2	–
720	3.193e-3	0.75	7.525e-3	0.81
1440	1.668e-3	0.94	3.885e-3	0.95
2880	8.656e-4	0.94	1.975e-3	0.97

- As noted by Woodward & Colella (1984), Roberts (1990), and Quirk (1994) downstream long-wavelength oscillations are present for very slowly moving shock waves
- Roberts concludes that a differentiable form of the numerical flux construction appears necessary to remove these
- $\frac{1}{S(\mathbf{u}^\epsilon)}\partial_t C^\epsilon - \gamma\partial_x^2 C^\epsilon + \frac{1}{\epsilon}C^\epsilon = G(\partial_x u^\epsilon)$ – allow γ depend inversely on Mach number

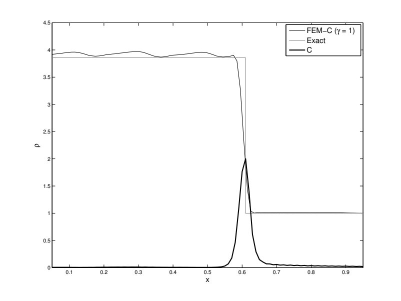

(g) $\gamma = 1$

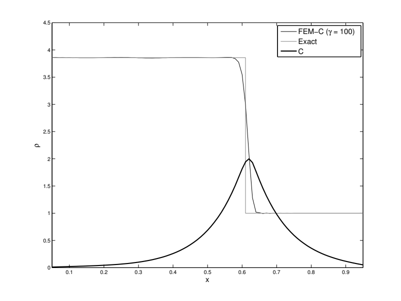

(h) $\gamma = 100$

Figure 7: FEM-C for a very slowly moving shock

The C-Method in Multi-D

Description for the 2-D compressible Euler equations

- Shock waves: $[[u \cdot n]] \neq 0$ and $[[u \cdot \tau]] = 0$ on $\Gamma(t)$
- Contact discontinuities: $[[u \cdot n]] = 0$ and $[[u \cdot \tau]] \neq 0$ on $\Gamma(t)$
- For simplicity, first assume that $\Gamma(t)$ is y-axis
  - $n = (1,0)$ and $\tau = (0,1)$
- In this case, the C-method is given by

$$\partial_t(\rho u^1) + (\rho u^1 u^j + p\delta^{1j})_{,j} = \beta_u \epsilon^2 [A^{rs}(\rho u^1)_{,s}]_{,r}$$

$$\partial_t(\rho u^2) + (\rho u^2 u^j + p\delta^{2j})_{,j} = \beta_u \epsilon^2 [A^{rs}(\rho u^2)_{,s}]_{,r}$$

$$\partial_t \rho + (\rho u^i)_{,i} = \epsilon^2 \beta_\rho [(C_1^1 + C_1^2)\rho_{,1}]_{,1}$$

$$\partial_t E + [(E+p)u^i]_{,i} = \epsilon^2 \beta_E [(C_1^1 + C_1^2)E_{,1}]_{,1}$$

where

$$A^{kl} = \sqrt{C_k^i C_l^i} \quad \text{(no sum on } i\text{)}$$

and C_j^i satisfy the matrix C-equation

$$\frac{1}{S(\mathbf{u})}\partial_t C_j^i - \gamma \Delta C_j^i + \frac{1}{\epsilon} C_j^i = \mathbf{1}_{\operatorname{div} u<0} \frac{|u^i{}_{,j}|}{\max |u^i{}_{,j}|}$$

The C-Method in Multi-D

Description for the 2-D compressible Euler equations

- Now for a moving $\Gamma(t)$ with time-dependent n and τ, set $Q = \begin{bmatrix} n^1 & n^2 \\ \tau^1 & \tau^2 \end{bmatrix}$
- In this setting, the matrix C is a smoothed version of $\begin{bmatrix} \partial_n(u \cdot n) & \partial_\tau(u \cdot n) \\ \partial_n(u \cdot \tau) & \partial_\tau(u \cdot \tau) \end{bmatrix}$ and n is found my *maximizing* the function $\|\nabla u(x,t) \cdot n(x,t)\|_{l^2}$
- The C-method takes the following form

$$\partial_t(\rho u^i) + \frac{\partial}{\partial x^j}\left(\rho u^i u^j + p\delta^{ij}\right) = \epsilon^2 \beta_u \left\{ Q_{1i} Q_{mr} \frac{\partial}{\partial x^r}\left[A_1^{mq} \rho Q_{qs} \frac{\partial}{\partial x^s}\left(Q_{1j} u^j\right)\right] + Q_{2i} Q_{mr} \frac{\partial}{\partial x^r}\left[A_2^{mq} \rho Q_{qs} \frac{\partial}{\partial x^s}\left(Q_{2j} u^j\right)\right] \right\}$$

$$\partial_t \rho + \frac{\partial}{\partial x^i}(\rho u^i) = \epsilon^2 \beta_\rho Q_{1i} \frac{\partial}{\partial x^i}\left[(C_1^1 + C_1^2) Q_{1j} \frac{\partial \rho}{\partial x^j}\right]$$

$$\partial_t E + \frac{\partial}{\partial x^i}\left[(E + p) u^i\right] = \epsilon^2 \beta_E Q_{1i} \frac{\partial}{\partial x^i}\left[(C_1^1 + C_1^2) Q_{1j} \frac{\partial E}{\partial x^j}\right]$$

where

$$\frac{1}{S(\mathbf{u})} \partial_t C_j^i - \gamma \Delta C_j^i + \frac{1}{\epsilon} C_j^i = \mathbf{1}_{\operatorname{div} u < 0} \frac{|Q_{jk}(Q_{il} u^l)_{,k}|}{\max |Q_{js}(Q_{ir} u^r)_{,s}|}$$

Convergence to Entropy Solution

- Consider the isentropic Euler equations: for $\gamma > 1$,

$$\begin{aligned} (\rho u)_t + (\rho^{-1} m^2 + p)_x &= 0, \\ \rho_t + (\rho u)_x &= 0\,, \\ p(\rho) &= \rho^\gamma\,. \end{aligned}$$

- The C-method regularization is given by

$$\begin{aligned} m_t^\epsilon + [(m^\epsilon)^2/\rho^\epsilon + p^\epsilon]_x &= \epsilon^2 [C^{\epsilon,\delta} m_x^\epsilon]_x, \\ \rho_t^\epsilon + m_x^\epsilon &= \epsilon^2 (C^{\epsilon,\delta} \rho_x)_x\,, \\ p^\epsilon(\rho^\epsilon) &= (\rho^\epsilon)^\gamma\,, \\ C_t^\epsilon - S(u^\epsilon) C_{xx}^\epsilon + \frac{S(u^\epsilon)}{\epsilon} C^\epsilon &= S(u^\epsilon) G(u_x^\epsilon)\,. \end{aligned}$$

- Basic energy law

$$\begin{aligned} &\frac{d}{dt}\left[\int \frac{1}{2}\rho^\epsilon (u^\epsilon)^2\, dx + \frac{1}{\gamma - 1}\int p^\epsilon\, dx\right] \\ &\qquad = -\epsilon^2 \int C^{\epsilon,\delta} \rho^\epsilon\, (u_x^\epsilon)^2\, dx - \epsilon^2 \gamma \int C^{\epsilon,\delta} (\rho^\epsilon)^{\gamma-2} (\rho_x^\epsilon)^2\, dx\,. \end{aligned}$$

Convergence to Entropy Solution

Continued

- For $\epsilon > 0$, solutions to C-method are smooth (H^3 regularity a.e. t)
- The functions $\eta, q : \mathbb{R}^2 \to \mathbb{R}$ are called an entropy-flux pair if additional conservation law satisfied:

$$\eta(\mathbf{u})_t + q(\mathbf{u})_x = 0$$

  which holds off

$$\nabla \eta(\mathbf{u}) \nabla f(\mathbf{u}) = \nabla q(\mathbf{u})\,.$$

- A weak solution is the unique entropy solution if

$$\eta(\mathbf{u})_t + q(\mathbf{u})_x \leq 0\,.$$

- For isentropic gas dynamics, the total energy is an entropy function:

$$\eta(m, \rho) = \frac{m^2}{2\rho} + \frac{\rho^\gamma}{\gamma - 1}$$

- $\nabla^2 \eta(m, \rho)$ is positive whenever $\rho > 0$.

Convergence to Entropy Solution

Continued

- Taking the inner-product of $\nabla\eta(\mathbf{u}^\epsilon)$ with C-method

$$\eta(\mathbf{u}^\epsilon)_t + q(\mathbf{u}^\epsilon)_x = \epsilon^2 \nabla\eta(\mathbf{u}^\epsilon)\,[\mathcal{C}\mathbf{u}^\epsilon_x]_x$$
$$= \epsilon^2\,[\mathcal{C}\eta(\mathbf{u}^\epsilon)_x]_x - \epsilon^2 [\mathbf{u}^\epsilon_x]^T\,\mathcal{C}\,\nabla^2\eta(\mathbf{u}^\epsilon)\mathbf{u}^\epsilon_x\,.$$

- Integrating over the spatial domain and then over the time interval $[0, T]$ yields

$$\int \eta(\mathbf{u}^\epsilon(x,T))dx - \int \eta(\mathbf{u}^\epsilon(x,0))dx = -\epsilon^2 \int_0^T \int [\mathbf{u}^\epsilon_x]^T\,\mathcal{C}\,\nabla^2\eta(\mathbf{u}^\epsilon)\mathbf{u}^\epsilon_x\,dx\,dt\,,$$

- from which it follows that

$$\int_0^T \int |\epsilon\mathbf{u}^\epsilon_x|^2\,dx\,dt \le \bar{c}$$

Convergence to Entropy Solution

Continued

- For a smooth, non-negative test function ψ with compact support in the strip $\mathcal{I} \times (0, T)$,

$$\iint \eta(\mathbf{u}^\epsilon \phi_t + q(\mathbf{u}^\epsilon)\phi_x \, dxdt = \epsilon \iint \mathcal{C}(\epsilon \mathbf{u}^\epsilon)_x \phi_x \, dxdt + \iint \epsilon^2 [\mathbf{u}_x^\epsilon]^T \mathcal{C} \, \nabla^2 \eta(\mathbf{u}^\epsilon) \mathbf{u}_x^\epsilon \phi \, dxdt \, .$$

- first term on the right-hand side goes to zero like ϵ, while the second term is non-negative, since $\nabla^2 \eta$ is positive-definite
- as $\epsilon \to 0$, we recover the entropy inequality
- Switching to Riemann invariants provides bounds on the amplitude of solutions
- Compensated compactness of DiPerna (1983) and Lions, Perthame, & Souganidis (1996) gives pointwise convergence
- Maximum principle arguments show density is bounded away from vacuum

Conclusions

- We have proven that for isentropic Euler, smooth solutions of the *C*-method converge to the unique entropy solution as $\epsilon \to 0$
- For general gas dynamics, the proof of Bianchini and Bressan (2005) can be adapted to reach the same conclusion
- The *C*-method preserves the basic symmetries of the Euler equations
- Performs better than classical artificial viscosity, and maintains the order of accuracy of the underlying higher-order numerical method
- A natural multi-D extension exists, which is provably convergent to *shock-front* solutions for short-time
- Fairly easy to implement and ensures the convergence of approximate Riemann solvers to the correct entropy solution as discussed by Roberts (1990)
- Ideal for complex physics with memory effects and non-convex equations of state, modeled by hyperbolic systems which are not genuinely nonlinear and/or linearly degenerate.

Conclusions

- We have proven that for isentropic Euler, smooth solutions of the *C*-method converge to the unique entropy solution as $\epsilon \to 0$
- For general gas dynamics, the proof of Bianchini and Bressan (2005) can be adapted to reach the same conclusion
- The *C*-method preserves the basic symmetries of the Euler equations
- Performs better than classical artificial viscosity, and maintains the order of accuracy of the underlying higher-order numerical method
- A natural multi-D extension exists, which is provably convergent to *shock-front* solutions for short-time
- Fairly easy to implement and ensures the convergence of approximate Riemann solvers to the correct entropy solution as discussed by Roberts (1990)
- Ideal for complex physics with memory effects and non-convex equations of state, modeled by hyperbolic systems which are not genuinely nonlinear and/or linearly degenerate.

Conclusions

- We have proven that for isentropic Euler, smooth solutions of the *C*-method converge to the unique entropy solution as $\epsilon \to 0$
- For general gas dynamics, the proof of Bianchini and Bressan (2005) can be adapted to reach the same conclusion
- The *C*-method preserves the basic symmetries of the Euler equations
- Performs better than classical artificial viscosity, and maintains the order of accuracy of the underlying higher-order numerical method
- A natural multi-D extension exists, which is provably convergent to *shock-front* solutions for short-time
- Fairly easy to implement and ensures the convergence of approximate Riemann solvers to the correct entropy solution as discussed by Roberts (1990)
- Ideal for complex physics with memory effects and non-convex equations of state, modeled by hyperbolic systems which are not genuinely nonlinear and/or linearly degenerate.

Conclusions

- We have proven that for isentropic Euler, smooth solutions of the *C*-method converge to the unique entropy solution as $\epsilon \to 0$
- For general gas dynamics, the proof of Bianchini and Bressan (2005) can be adapted to reach the same conclusion
- The *C*-method preserves the basic symmetries of the Euler equations
- Performs better than classical artificial viscosity, and maintains the order of accuracy of the underlying higher-order numerical method
- A natural multi-D extension exists, which is provably convergent to *shock-front* solutions for short-time
- Fairly easy to implement and ensures the convergence of approximate Riemann solvers to the correct entropy solution as discussed by Roberts (1990)
- Ideal for complex physics with memory effects and non-convex equations of state, modeled by hyperbolic systems which are not genuinely nonlinear and/or linearly degenerate.

Conclusions

- We have proven that for isentropic Euler, smooth solutions of the *C*-method converge to the unique entropy solution as $\epsilon \to 0$
- For general gas dynamics, the proof of Bianchini and Bressan (2005) can be adapted to reach the same conclusion
- The *C*-method preserves the basic symmetries of the Euler equations
- Performs better than classical artificial viscosity, and maintains the order of accuracy of the underlying higher-order numerical method
- A natural multi-D extension exists, which is provably convergent to *shock-front* solutions for short-time
- Fairly easy to implement and ensures the convergence of approximate Riemann solvers to the correct entropy solution as discussed by Roberts (1990)
- Ideal for complex physics with memory effects and non-convex equations of state, modeled by hyperbolic systems which are not genuinely nonlinear and/or linearly degenerate.

Future Directions

- Use C-method to generalize sub-grid stress models such as LES, RANS, k-ϵ, etc. Spacetime filtering should perform better than space filtering, and allow for *naturally adjusting scales*.
- In multi-D, C must provide anisotropic smoothing, naturally weighted to contacts and shocks, and combinations which occur during collisions – connections with covariance fluctuation tensor, micro-scale physics
- Multi-D transport with reaction physics – develop *noise detectors* using decay of polynomial modes in higher-order schemes such as DG
- Without reliance on dimensional splitting and Riemann solvers, easy to couple gas dynamics and plasmas with incompressible flow, nonlinear solid dynamics, and systems with multiple phases.

Future Directions

- Use C-method to generalize sub-grid stress models such as LES, RANS, k-ϵ, etc. Spacetime filtering should perform better than space filtering, and allow for *naturally adjusting scales*.
- In multi-D, C must provide anisotropic smoothing, naturally weighted to contacts and shocks, and combinations which occur during collisions – connections with covariance fluctuation tensor, micro-scale physics
- Multi-D transport with reaction physics – develop *noise detectors* using decay of polynomial modes in higher-order schemes such as DG
- Without reliance on dimensional splitting and Riemann solvers, easy to couple gas dynamics and plasmas with incompressible flow, nonlinear solid dynamics, and systems with multiple phases.

Future Directions

- Use C-method to generalize sub-grid stress models such as LES, RANS, k-ϵ, etc. Spacetime filtering should perform better than space filtering, and allow for *naturally adjusting scales*.
- In multi-D, C must provide anisotropic smoothing, naturally weighted to contacts and shocks, and combinations which occur during collisions – connections with covariance fluctuation tensor, micro-scale physics
- Multi-D transport with reaction physics – develop *noise detectors* using decay of polynomial modes in higher-order schemes such as DG
- Without reliance on dimensional splitting and Riemann solvers, easy to couple gas dynamics and plasmas with incompressible flow, nonlinear solid dynamics, and systems with multiple phases.